Available online at www.sciencedirect.com
ScienceDirect
Journal of Power Sources 171 (2007) 489–494
JOURNAL OF POWER SOURCES
www.elsevier.com/locate/jpowsour

Short communication

Effects of anode surface modification on the performance of low temperature SOFCs

Na Ai [a], Zhe Lü [a,*], Kongfa Chen [a], Xiqiang Huang [a], Xiaobo Du [b], Wenhui Su [a,b,c]

[a] *Center for Condensed Matter Science and Technology, Harbin Institute of Technology, Harbin 150001, China*
[b] *Department of Condensed Matter Physics, Jilin University, Changchun 130022, China*
[c] *International Center for Material Physics, Academia, Shenyang 110015, China*

Received 4 June 2007; accepted 11 June 2007
Available online 23 June 2007

Abstract

An anode functional layer (AFL, ~5 μm) for improving the cell performance was fabricated by the slurry spin coating method on the porous surface of an anode substrate. The effects of the AFL on the anode/electrolyte interfacial morphology and the $Sm_{0.2}Ce_{0.8}O_{1.9}$ (SDC) film deposition process were evaluated. And the electrochemical characteristics of the cells with and without the AFL were tested for comparison. With the AFL layer, the cell performance was greatly improved and the maximum power density was increased from 0.733 to 0.884 W cm^{-2} at 600 °C and from 1.085 to 1.213 W cm^{-2} at 650 °C. The systematical analysis indicated that the AFL could effectively reduce the anode polarization loss by increasing the three-phase boundary (TPB) length.

Keywords: Solid oxide fuel cell; Anode functional layer (AFL); Three-phase boundary (TPB); Slurry spin coating; $Sm_{0.2}Ce_{0.8}O_{1.9}$ (SDC)

1. Introduction

Solid oxide fuel cell (SOFC) has attracted more and more attentions due to its merits such as a high energy conversion efficiency, a low noise and a low greenhouse emission [1,2]. Nickel (Ni) has been usually adopted as an anode material in SOFC because of its high catalytic activity for the fuel oxidation and their reasonable cost [2]. The particle size of NiO has a great effect on determining the effective reaction zone (ERZ) in an anode. Suzuki et al. [3] reported that the micro-sized NiO powders were not suitable in the case of increasing the three-phase boundary (TPB) around the gas/anode/electrolyte interfaces, which was very vital for the anode electrochemical activity. Whereas, the submicro-sized NiO particles could increase the TPB as well as bringing a problem of low porosity, which could lead to a relatively slow diffusion of reactant and resultant in the anode, and thus limit the overall reaction rate [4]. Therefore, in the present study submicro-sized NiO was adopted while wheat flour was added as a pore-former in the anode to form a suitable porosity. However, the pore-former usually leads to a porous anode surface. According to Horita et al.'s study [5], the surface properties of anode metals and oxide electrolytes could affect the anodic reaction mechanism and kinetics around the interfaces. In addition, the anode surface property could affect the fabrication process of electrolyte film. Therefore, the pore structure of the anode substrate has to be characterized and modified.

To design the anode/electrolyte interface appropriately, many studies had been done on an anode functional layer (AFL) on the porous anode substrate, which could control the surface roughness and pore size of the anode substrate, resulting in the increased TPB and the reduced interfacial polarization losses [6–8]. However, the investigations of the AFL in most of these researches correlated with the commonly used NiO/YSZ (yttria-stabilized zirconia) anode. The study of the AFL properties in low temperature SOFC based on a doped ceria film is not sufficient. Moreover, in previous studies the AFL film usually required an additional pre-firing step before the fabrication of the electrolyte film [7,8], which makes the process more complicated and energy-consuming.

In this paper, we fabricated the AFL without any intermediate firing step for the low temperature SOFC based on the

* Corresponding author. Tel.: +86 451 86418420; fax: +86 451 86412828.
E-mail addresses: ina396@163.com (N. Ai), lvzhe@hit.edu.cn (Z. Lü).

0378-7753/$ – see front matter © 2007 Elsevier B.V. All rights reserved.
doi:10.1016/j.jpowsour.2007.06.055

samaria-doped ceria ($Sm_{0.2}Ce_{0.8}O_{1.9}$, SDC) film. The effects of AFL on the electrolyte film fabrication process and the cell performance were investigated. The electrochemical properties of the cells were also presented and discussed.

2. Experimental

Nickel oxide (NiO) powders were synthesized by the precipitation method and calcined at 400 °C for 2 h. The average crystallite size of NiO was 20–30 nm and the average size of its agglomerate particles was about 0.36 μm [4]. Samaria-doped ceria ($Sm_{0.2}Ce_{0.8}O_{1.9}$, SDC) powders were prepared using the glycine-nitrate process (GNP) and calcined at 800 °C for 2 h. The average crystallite size of SDC was 30 nm and the average size of the secondary particles was about 0.2 μm after ball-milling [9]. NiO, SDC and wheat flour in a weight ratio of 52.9:28.5:18.6 were pestled in a mortar for 2 h to form the green anode powders. The anode powders were then compressed into pellets with a diameter of 13 mm and sintered at 950 °C to get the green anode substrates (Anode-1).

An anode functional layer (AFL) was deposited on one side of the anode disk with an anode slurry containing NiO, SDC and binder in the weight ratio 21.7:11.7:66.6. The binder was consisted of ethyl cellulose (chemical reagent) and terpineol (analytical reagent) in a weight ratio of 5.5:94.5. After the anode with an AFL (denoted as Anode-2) was heated at 400 °C for 10 min, an SDC electrolyte film was directly coated on the AFL surface and then co-sintered at 1400 °C for 4 h. The SDC slurry was obtained by mixing the SDC powders and the binder in a weight ratio of 25:75. The AFL (NiO/SDC) and the SDC film were both fabricated using the slurry spin coating method [9] with a spinning rate of 6k rpm for 60 s. For comparison, we also fabricated an SDC film on the Anode-1 substrate. The cathode slurry containing $Ba_{0.5}Sr_{0.5}Co_{0.8}Fe_{0.2}O_{3-\delta}$ (BSCF) powders and terpineol was applied on the SDC film, followed by sintering at 1050 °C for 4 h to form the porous cathode layer. The cells based on Anode-1 and Anode-2 were denoted as Cell-1 and Cell-2, respectively. The diameter of the cell was 1.04 cm after sintering and the cathode area was 0.06 cm^2. A silver paste (DAD-87, Shanghai Research Institute of Synthetic Resin) was painted onto the electrodes surface and then heated to form the current collectors.

After the reduction of the NiO anode in H_2 at 600 °C, the electrochemical properties of the cells were tested with a four-probe method. 30 ml min^{-1} hydrogen as the fuel was fed to the anode side and the stationary air was used as the oxidant. The output performance and AC impedance spectra of the cells were measured with electrochemical interface Solartron SI 1287 and impedance analyzer SI 1260. Scanning electron microscopes (SEM), Hitachi S-570 and JEOL JSM 6480LV, were used to reveal the microstructure of the samples.

3. Results and discussion

Fig. 1a presents the surface microstructure of Anode-1. There were many big pores with different sizes (3–20 μm) on the surface. It illustrated that the organic pore-former powders were seriously aggregated and inhomogeneously distributed in the green anode, resulting in the created pores with irregular shape and cracks imprinted on the anode surface. And from the SEM images of the anode structure after sintering, the size of the flour agglomerate was presumed to be 3–20 μm. As also observed, there were some small isolated anode parts in the big pores and holes, suggesting that the NiO/SDC anode powders were absolutely covered by the flour powders during milling. These pores and the isolated anode structures on the anode surface would affect the interfacial properties between the electrolyte and anode substrate. As shown in Fig. 1b, it was found that the pores near the interface were partly filled or bridged over by the SDC electrolyte film after co-sintering at 1400 °C.

In an attempt to explain this phenomenon, schemes of different interfacial conditions during the film fabrication process

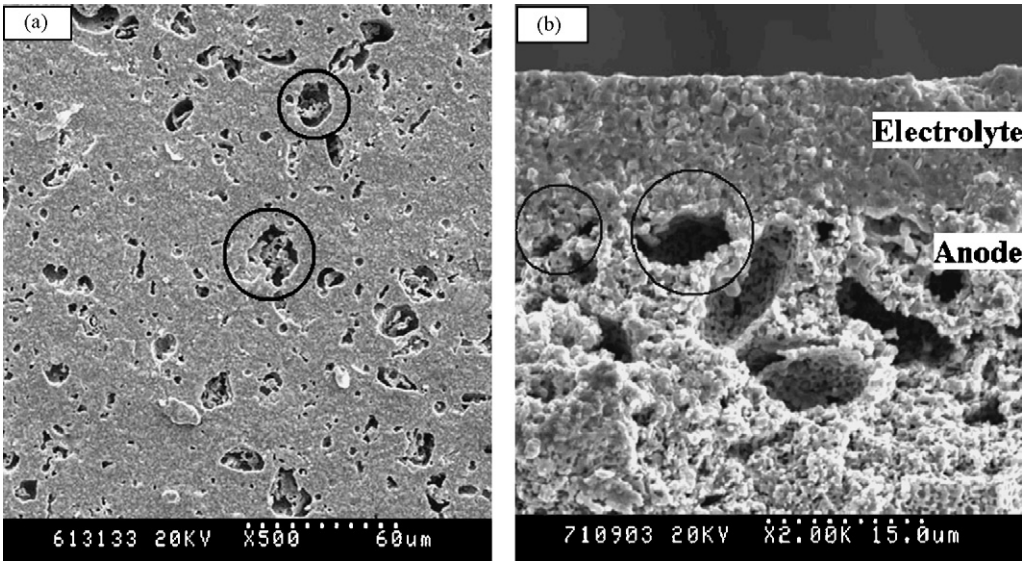

Fig. 1. SEM micrographs of (a) the surface of Anode-1 before reduction and (b) interfacial structure between the SDC film and Anode-1.

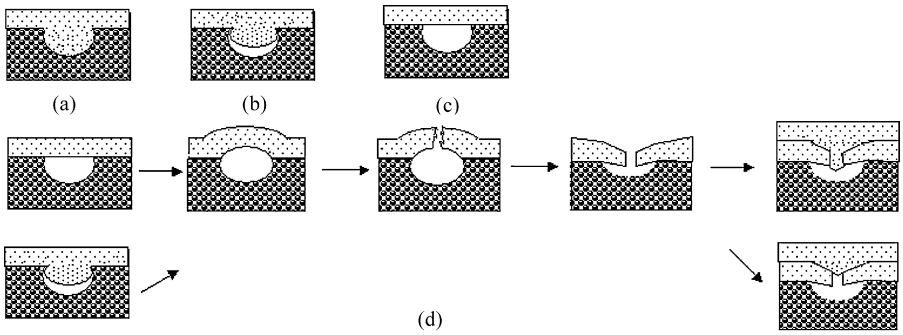

Fig. 2. The models for the contact between the SDC film and the defect on the anode surface: (a) electrolyte slurry fills the defect fully; (b) electrolyte slurry fills the defect partly; (c) electrolyte slurry bridges on the defect; (d) the changing in the baking process (anode, electrolyte).

on Anode-1 are presented in Fig. 2. If the electrolyte slurry filled the defects fully, as shown in Fig. 2a, the negative influence of the defect on the interfacial contact could be diminished. When the pores were not filled up by the electrolyte as shown in Fig. 3b and c, the existence of pores at the interface would restrict the ionic or electronic conduction paths and increase the anode polarization [6,7]. Besides, the large pores would reduce the amount of TPB because the anode particles could otherwise have been presented in the locations of the pores [10]. The defects on the Anode-1 surface might also bring some problems during the heating process as imagined and described in Fig. 2d. In the process of fabricating the SDC film, the organic additive in one coating was removed by a heat-treatment before the next coating. However, in the heating process the gas trapped inside the pores might expand and push the SDC film, forming some pores and cracks in the films [11]. Then the broken film might possibly sink into the pores in the anode. Though the defects left on the former layer could be partly repaired after coating the latter layer, some defects still exist in the electrolyte film, which are not beneficial for obtaining a dense SDC film. As the contact area decreases, the mechanical strength of the cell would be reduced, which is disadvantageous for long-term operation [12]. Therefore, the defects on the anode surface left by burnout of the pore-formers not only might decrease the TPB near the anode/electrolyte interface but also cause a failure in the film fabrication and cell testing processes.

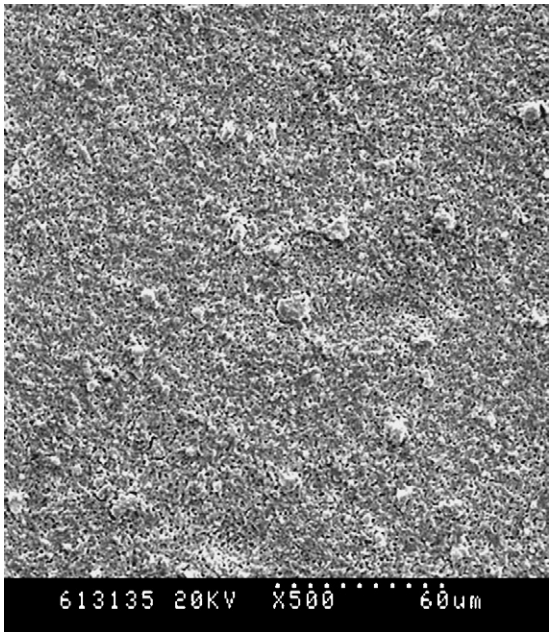

Fig. 3. SEM micrograph of the surface of Anode-2 before reduction.

Shown in Fig. 3 is the surface morphology of Anode-2. After deposition of the AFL, large pores in the Anode-1 surface disappeared, as compared with Fig. 2a. It suggested that the defects on the anode surface could be significantly eliminated by the surface modification. And some grains aggregated by the anode powders in the slurry were distributed on the Anode-2 surface, which could maintain the roughness of the interface of anode/electrolyte, and thus increase the adhesion between the two components. The cross-sectional views of Cell-1 and Cell-2 are shown in Fig. 4. As presented in Fig. 4b, the AFL structure well connected the anode substrate structure to the SDC film. And the distribution of the small pores was uniform and the porosity of AFL was much lower than that of the anode substrate. So, the TPB at the anode/SDC interface was substantially increased due to the lower porosity and the smaller pore size of the AFL. Also, the problems brought by the pore-formers in the fabrication process of SDC film as mentioned above were solved.

In Cell-1, through the large pore area at the interface of anode/electrolyte, the fuel could directly reach and impact the SDC film. This effect was harmful for the mechanical strength of the thin electrolyte film, which was disadvantageous for long-term operation. On the other hand, in Cell-2, the smaller pores in the AFL structure could restrict the disadvantage of fuel impact. Therefore, the AFL structure could greatly enhance the stability of the electrolyte film and the system.

From Fig. 4, it was known that the average thicknesses of the SDC film of Cell-1 and Cell-2 were 19 and 20 μm, respectively. The AFL structure on the anode substrate was clearly visible, and was about 5 μm thick after one time coating by the slurry spin coating method. Basu et al.'s [7] reported that a minimum of seven layers were required to build up a 6-μm-thick AFL by the wet powder spraying method, which was more complicated and time-consuming. Moreover, the AFL fabrication in this study avoids the additional firing process, which is quite fast and cost-effective.

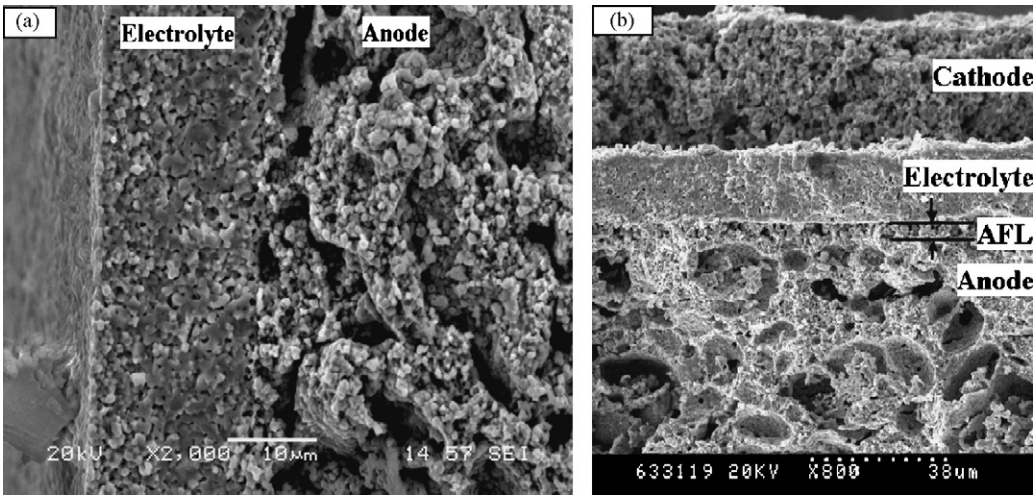

Fig. 4. SEM micrographs of the cross-sectional view of (a) Cell-1 and (b) Cell-2.

Fig. 5 illustrates the electrochemical characteristics of Cell-1 and Cell-2 at different temperatures. The maximum power densities (MPDs) are listed in Table 1. Obviously, the performance of Cell-2 was better than that of Cell-1, which was attributed to the effect of the AFL. The *I–V* curves of Cell-1 and Cell-2 at 600 °C were very close at the low current density region and became quite different with the increased current density. The voltage drop of Cell-1 with the current density was much faster than that of Cell-2, typically when the current density was higher than 1.8 A cm^{-2}. Moreover, the open-circuit voltage (OCV) of Cell-2 (0.81 V) was a little higher than that of Cell-1 (0.79 V).

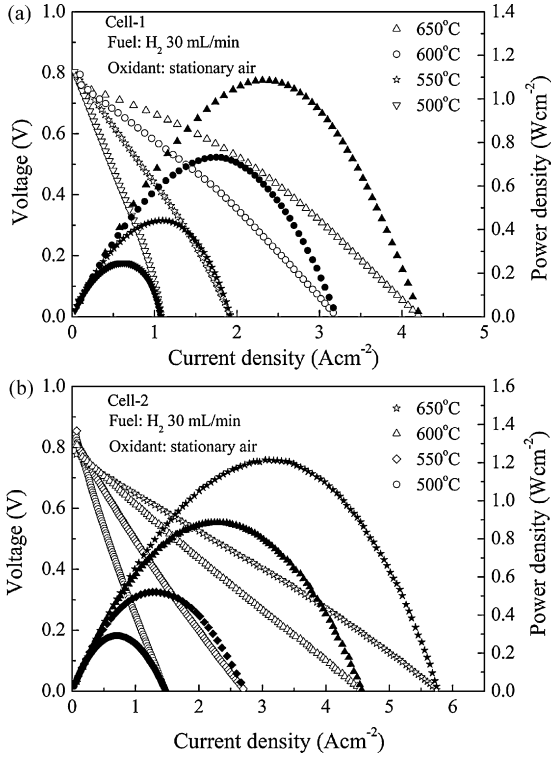

Fig. 5. Voltage and power density vs. current density at various temperatures of (a) Cell-1 and (b) Cell-2.

Table 1
Maximum power densities and their promotion ratios at different temperatures

	Temperature (°C)			
	650	600	550	500
MPD of Cell-1 (W cm^{-2})	1.085	0.733	0.441	0.248
MPD of Cell-2 (W cm^{-2})	1.213	0.884	0.521	0.292
Promotion ratio (%)	11.8	20.6	18.1	17.7

The possible reason was that there was gas leakage through the electrolyte film of Cell-1. So, it demonstrates that the AFL actually has a positive effect on the quality of the SDC film, in accordance with the discussion in Fig. 2.

Fig. 6 displays the impedance spectra of the two cells measured at 600 °C under the open circuit conditions. The intercept on the real axis at high frequency region represented the total ohmic resistance of the cell. The ohmic resistance of Cell-2 was 0.078 Ω cm^2, a little higher than that of Cell-1, 0.058 Ω cm^2. The total ohmic resistance includes the ohmic resistance of the electrolyte film, the ohmic resistance of the electrodes and the contact resistances between each neighboring cell components. From the observation of Fig. 4, the thickness of the SDC film of Cell-2 was about 1 μm thicker than that of Cell-1. Besides

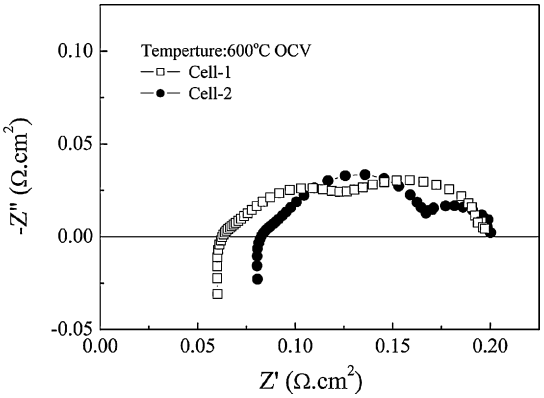

Fig. 6. Impedance spectra of Cell-1 and Cell-2 measured at 600 °C under open circuit conditions.

the various kinds of ohmic resistances of Cell-1, the total ohmic resistance of Cell-2 contains the ohmic resistance of the AFL and the contact resistances around the anode substrate/AFL/SDC film interfaces in addition. Therefore, it could be deduced that the increased total ohmic resistance was possibly related to the thicker SDC film and the increased contact resistance brought by the AFL. The electrode polarization resistances of Cell-1 and Cell-2 were 0.14 and 0.12 $\Omega\,cm^2$, respectively. The electrode polarization resistance includes the anode polarization resistance and the cathode polarization resistance. And the polarization of anode is related to the resistance for the movements of reaction gases and ions around the TPB [2]. The AFL structure increased the amount of TPB and thus enhanced the electrochemical reaction rate and the exchange current density, leading to a better anode performance.

To further analyze the reasons for the improvement of cell performance, the contributions of the ohmic and the electrode polarization losses were evaluated based on the cell impedance spectra measured under different voltages. As shown in Fig. 7, the ohmic resistance of the two cells both increased with the decreasing cell voltage. And the electrode polarization resistance of Cell-1 increased with the decreasing cell voltage. On the contrary, the value of electrode polarization resistance of Cell-2 kept increasing when the cell voltage was higher than 0.4 V, and then decreased with the cell voltage.

Fig. 8 displays the ohmic and electrode polarization losses versus current density for the two cells at 600 °C. The electrode polarization was obtained through the *I–V* characteristics by subtracting the ohmic losses as derived from the impedance spectra (in Fig. 7). The ohmic loss of Cell-2 was a little higher than that of Cell-1, due to the higher ohmic resistance of Cell-2. On the other hand, at the same current density the electrode polarization of Cell-1 was much higher than that of Cell-2. Combination of the *I–V* curves is shown in Fig. 5, and it might be assumed that the anode concentration polarization restricted the output performance of Cell-1. It was proposed that the concentration polarization phenomenon originated from a combination of competitive adsorption near the reactive sites at the anode/electrolyte interface, followed by the surface diffusion to those sites [14]. However, it was rather surprising that the large pore size and high porosity of Anode-1 seemed to impede the fuel supply to the electrochemical active sites. On the contrary, from the observation of the *I–V* curve of Cell-2, it is found that sufficient gas flow could be supplied to the reaction sites for the efficient electrochemical reactions even after the surface modification. Even if the short-circuit current density was higher than that of Cell-1, there was still no concentration polarization phenomena in the *I–V* curve of Cell-2. So, the concentration polarization was not the cause for the higher electrode polarization of Cell-1. Because the faster reactant diffusion through the large pores of Cell-1, it was expected to have a lower electrode polarization associated with the gas transport process. However, the large pores in Cell-1 resulted in not only faster gas diffusion,

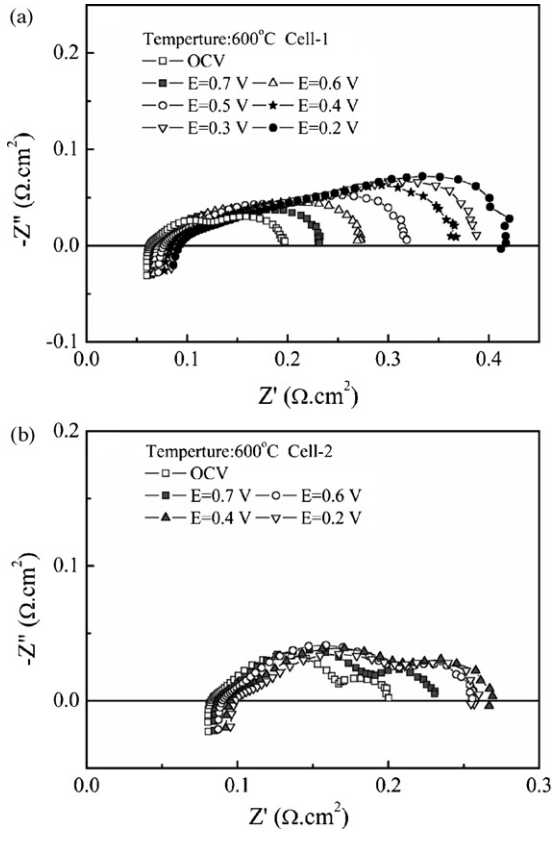

Fig. 7. Impedance spectra measured under different cell voltages of (a) Cell-1 and (b) Cell-2.

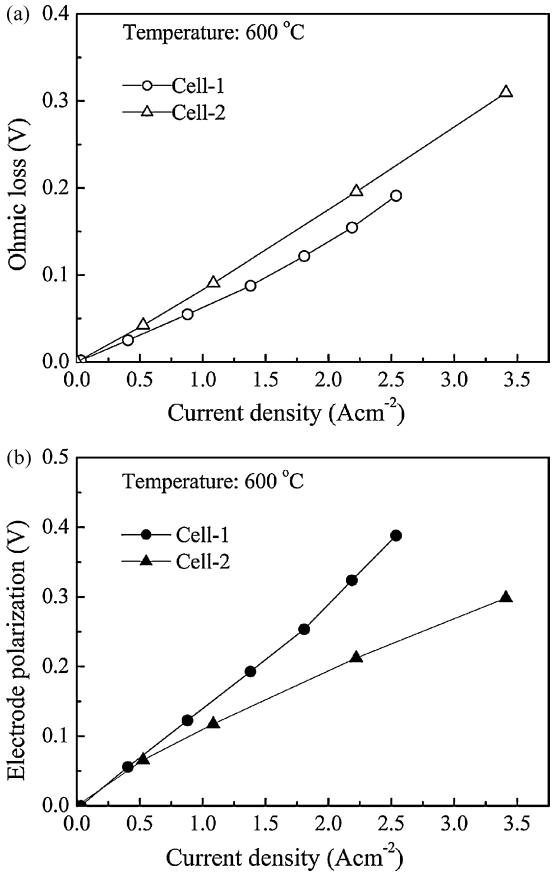

Fig. 8. (a) Ohmic loss vs. current density and (b) electrode polarization vs. current density at 600 °C.

but also a loss in TPB area for reaction. It is known that the performance of electrodes depends on a trade off between the TPB and the transport ability of the reactant in and the resultant out of the reaction area [13]. Therefore, when the performance improvement in gas diffusion was overwhelmed by the polarization associated with the loss of the active TPB, the electrode polarization of Cell-1 increased. On the other hand, in Cell-2, the reactant could diffuse to the reaction area through the large pores in the anode substrate and the small pores in the thin AFL, while the amount of TPB increased due to the AFL structure. Therefore, the electrode polarization of Cell-2 was much lower than that of Cell-1. And the output performance of Cell-2 was higher than that of Cell-1, though the ohmic loss of Cell-2 was a little higher than that of Cell-1. Because more TPBs were required for the reaction at high current density, the difference between the electrode polarizations of the two cells became bigger with the increasing current density. In a word, the 5 μm thick AFL in the present study could effectively enhance the cell performance by increasing the amount of TPB, without blocking the fast gas diffusion.

There was an effective anode thickness where the reaction occurs next to the electrolyte [15]. With the 5-μm-thick AFL structure, Cell-2 possessed more TPB and the concentration polarization did not happen in the operation. However, the promotion ratio of the MPD at 650 °C was much smaller than that at 600, 550 and 500 °C (see Table 1). It could be assumed that the TPB was not enough for the reaction at 650 °C, which is related to the point that more TPB is required to obtain the higher current density. Increasing the thickness of the AFL could further enhance the amount of TPB. Then the porosity should be increased in order to maintain the sufficient gas diffusion for the reaction. It is believed that a better cell performance could be achieved by adjusting the thickness of AFL and the porosity of the anode substrate in the further investigation.

4. Conclusions

In this investigation, an anode functional layer (AFL, ∼5 μm thick) and an SDC film were deposited by the slurry spin coating technique to modify the anode/electrolyte interface. The microstructure of the anode/electrolyte interface illustrated that the AFL structure not only improved the interfacial connection and the electrolyte mechanical property but also avoided some problems in the fabrication of a SDC film. The *I–V* curves combined with the impedance spectra data suggested that the AFL could effectively reduce the electrode polarization by increasing the amount of TPB. Therefore, the cell performance was greatly improved and the maximum power density was increased from 0.733 to 0.884 W cm^{-2} at 600 °C and from 1.085 to 1.213 W cm^{-2} at 650 °C due to the existence of the AFL structure. Moreover, it is believed that a better cell performance can be expected by adjusting the thickness of AFL and the porosity of anode substrate in the further investigation.

Acknowledgement

The authors gratefully acknowledge the financial supports from the Ministry of Science and Technology of China 363 under contract no. 2001AA323090.

References

[1] Z.S. Duan, M. Yang, A.Y. Yan, Z.F. Hou, Y.L. Dong, Y. Chong, M.J. Cheng, W.S. Yang, J. Power Sources 160 (2006) 57–64.
[2] N.Q. Minh, J. Am. Ceram. Soc. 76 (3) (1993) 563–568.
[3] S. Suzuki, H. Uchida, M. Watanabe, Solid State Ionics 177 (2006) 359–365.
[4] K.F. Chen, Z. Lü, X.J. Chen, N. Ai, X.Q. Huang, B. Wei, J.Y. Hu, W.H. Su, J. Alloys Compd. (2007), doi:10.1016/j.jallcom.2006.12.130.
[5] T. Horita, H. Kishimoto, K. Yamaji, Y. Xiong, N. Sakai, M.E. Brito, H. Yokokawa, Solid State Ionics 177 (2006) 1941–1948.
[6] S.D. Kim, S.H. Hyun, J. Moon, J.-H. Kim, R.H. Song, J. Power Sources 139 (2005) 67–72.
[7] R.N. Basu, G. Blass, H.P. Buchkremer, D. Stöver, F. Tietz, E. Wessel, I.C. Vinke, J. Eur. Ceram. Soc. 25 (2005) 463–471.
[8] E. Wanzenberg, F. Tietz, P. Panjan, D. Stöver, Solid State Ionics 159 (2003) 1–8.
[9] N. Ai, Z. Lü, K.F. Chen, X.Q. Huang, Y.W. Liu, R.F. Wang, W.H. Su, J. Membr. Sci. 286 (2006) 255–259.
[10] J.J. Haslam, A.-Q. Pham, B.W. Chung, J.F. DiCarlo, R.S. Glass, J. Am. Ceram. Soc. 88 (2005) 513–518.
[11] K.F. Chen, Z. Lü, N. Ai, X.Q. Huang, Y.H. Zhang, X.D. Ge, X.S. Xin, X.J. Chen, W.H. Su, Solid State Ionics 177 (2007) 3455–3460.
[12] F. Gutierrez-Mora, J.M. Ralph, J.L. Routbort, Solid State Ionics 149 (2002) 177–184.
[13] V.V. Kharton, F.M.B. Marques, A. Atkinson, Solid State Ionics 174 (2004) 135–149.
[14] R.E. Williford, L.A. Chick, Surf. Sci. 547 (2003) 421–437.
[15] A. Abudula, M. Ihara, H. Komiyama, K. Yamada, Solid State Ionics 86–88 (1996) 1203–1209.